

Fog water flux at a canopy top: Direct measurement versus one-dimensional model

Otto Klemm^{*,1}, Thomas Wrzesinsky¹, Clemens Scheer²

University of Bayreuth, Bayreuth Institute for Ecosystem Research (BITÖK), Bayreuth, Germany

Received 9 August 2004; received in revised form 21 May 2005; accepted 25 May 2005

Abstract

A one-dimensional model [Lovett, 1984. Rates and mechanisms of cloud water deposition to a subalpine balsam fir forest. *Atmospheric Environment* 18, 361–371] to quantify fog water deposition was compared with results of long term (13 months) measurements of turbulent exchange with the eddy covariance method at a mountainous site in Central Europe. Turbulent exchange is mainly deposition and dominates over sedimentation at that site, therefore eddy covariance is a suitable tool in quantifying fog water deposition. The model can be operated with use of the measured droplet size distribution (DSD), with a DSD as parameterized from liquid water content (LWC) data, or with the measured visibility (VIS) as a quantitative indicator for fog. The latter is the easier measurement and therefore preferable for long-term applications. We compared the fog water deposition on a monthly basis. If VIS data are used as model input, the overall underestimate of the measurement is –23% as compared to the measurements. Using LWC and the parameterized DSD as input, the deviation is +37%. All deviations are highly significant.

© 2005 Elsevier Ltd. All rights reserved.

Keywords: Eddy covariance; Fog deposition; Liquid water content; Lovett model; Norway spruce

1. Introduction

The deposition of fog has long been recognized to be an important factor in the water balance of mountainous watersheds and ecosystems (Marloth, 1906; Linke, 1916; Grunow, 1955; Baumgartner, 1958, 1959). Fog is a cloud that is in physical contact with the surface. Two main processes lead to fog in mountainous regions. First, orographic lifting of air masses may lead to

cooling of the air below the cloud condensation point and thus favour the formation of fog. Secondly, a cloud may form in an air mass over terrain that is at lower altitudes a.s.l., be advected horizontally towards a mountain range, get into contact with the surface, and thus be a fog at this point. Because both processes are associated with advection of air masses, turbulent conditions are more likely to persist in mountain fogs than in radiation fogs, which are more typical for flat terrains and valleys. Therefore, turbulent transport is an important mechanism in the deposition of mountain fog water to the surface.

Various approaches have been applied to quantify the deposition of fog water through direct or indirect measurements: Mueller et al. (1991) measured canopy throughfall and stemflow, Lovett (1984) employed a fog collector resembling the natural surfaces, Trautner and

*Corresponding author.

E-mail address: oklemm@uni-muenster.de (O. Klemm).

¹Present address: University of Münster, Institute for Landscape Ecology (ILÖK), Robert-Koch-Str. 26, D-48149 Münster, Germany.

²Present address: Center of Development Research (ZEF), Department of Natural Resource Management, Bonn, Germany.

Eiden (1988) and Joslin et al. (1990) used living or artificial model trees, Fowler et al. (1990) employed a lysimeter to quantify fog deposition. Lacking spatial or temporal representativeness, and re-evaporation of deposited fog water before quantification, are possible sources of error in some of these approaches.

Lovett (1984) introduced a one-dimensional model to predict fog water deposition to a balsam fir forest. It uses data inputs of wind speed above the forest canopy, liquid water content, droplet size distribution, and various vegetation parameters, as drivers. The model has been widely applied and modified for various forests (Lovett and Reiners, 1986; Joslin et al., 1990; Mueller, 1991; Mueller et al., 1991; Pahl and Winkler, 1995; Pahl, 1996; US-EPA, 2000; Baumgardner et al., 2003) to predict turbulent deposition of fog water to mountainous forest ecosystems.

To our knowledge, the Lovett model has not been directly compared with eddy covariance measurements. In evaluations of simpler versions of the model with direct measurements Beswick et al. (1991) and Kowalski (1997) found reasonable agreement between the model and directly measured exchange, but the time periods for the inter-comparisons were very limited. We conducted quasi continuous measurements of turbulent exchange of fog by using the eddy covariance method for over a year in NE Bavaria (Wrzesinsky et al., 2004) and compare the results with the predictions of the one-dimensional Lovett model of fog deposition.

2. Material and methods

2.1. Site description

The experimental ecosystem research site *Waldstein* is within high altitudes of the *Fichtelgebirge* mountain range, NE Bavaria. This area was one of those with highest degree of forest decline symptoms in the 1980s. Acid precipitation and its impact on pollutant and nutrient cycling has been extensively studied in the 1980s (Schulze et al., 1989) and thereafter (Matzner, 2004). Due to reductions of the precursors of acid precipitation in Europe, steep decreases of the air concentrations of SO_2 (Klemm and Lange, 1999) and the acidity of fog (Wrzesinsky et al., 2004) since the middle 1980s could be observed.

The forest is dominated by planted Norway Spruce (*Picea abies* (L.) Karst.), with patches of stands of various age classes. A 30 m scaffolding walk-up tower is located at $50^\circ 08' 32'' \text{N}$, $11^\circ 52' 04'' \text{E}$, 775 m a.s.l in a terrain that slopes to the SSW with an angle of about 5° , and within a spruce stand that is up to 20 m high. The projected leaf area index (LAI) for the tower site was determined to be $5.3 \text{ m}^2 \text{ m}^{-2}$ (Alsheimer, 1996). From this number, the total leaf area (per ground area) can be

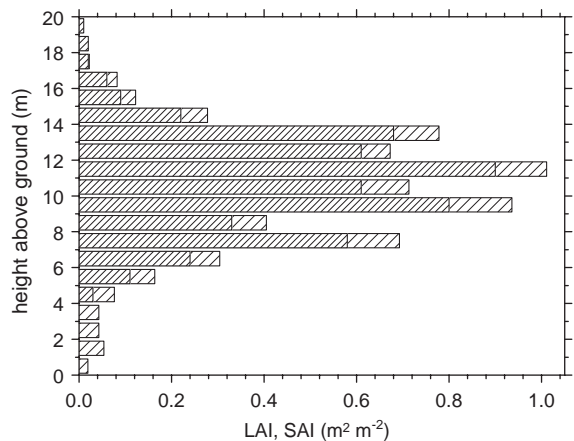


Fig. 1. Vertical distribution of the projected leaf area index (LAI, dark shaded bars) and the projected surface area index (SAI, dark plus light shaded bars) above ground at the Waldstein ecosystem research site (after Alsheimer, 1996; Tenhunen et al., 2001).

computed by multiplication with 2.57. The projected stem and twig area per ground area is $1.14 \text{ m}^2 \text{ m}^{-2}$. Assuming cylindrical stems and twigs, the total stem and twig area is computed as $1.14 \text{ m}^2 \text{ m}^{-2} \times \pi$. The total projected surface area index (SAI), including leaves, stems and twigs, is $(5.3 + 1.14) \text{ m}^2 \text{ m}^{-2}$. The distribution of LAI and SAI with altitude above ground is shown in Fig. 1.

Meteorological routine measurements have been performed at that tower since 1993. Radiation, air temperature, wind speed and direction are measured in 10-min averages at the tower top level. In addition, the wind speed profile is measured at heights of 2, 10, 16, 18, 21, 25, and 32 m a.g.l., respectively. The visibility (as measure for the presence and density of fog) is measured at 25 m a.g.l. with a Vaisala present weather detector PWD11.

During two experimental phases in 2000 and 2001/2002, respectively, physics and chemistry of fog were additionally measured. At 32 m a.g.l., an eddy covariance fog water exchange setup (Burkard et al., 2002; Thalmann et al., 2002; Wrzesinsky, et al., 2004) was installed. It was operated on an event basis and was triggered whenever the PWD11 measured a visibility below 1700 m. For these time periods, detailed information on the deposition flux of fog water to the forest is available. In addition, fog droplet size distributions are available with high temporal resolution for 40 size classes between 2 and $50 \mu\text{m}$ droplet diameter.

2.2. Deposition model

The one-dimensional cloud water deposition model was developed by Lovett (1984) and applied to a balsam

fir forest in the Appalachian Mountains. For our study, we used the version of Pahl and Winkler (1995), who modified it to use it in a mountain range with spruce forest in Germany. The deposition flux of fog water, F_{tot} , is predicted from the simple inferential model equation of the type

$$F_{\text{tot}} = \text{LWC} \times \frac{1}{R_{\text{tot}}}, \quad (1)$$

where LWC is the liquid water content in the foggy air, and R_{tot} is the total resistance against deposition. The forest is divided into layers of 1 m depth each, and R_{tot} is computed as a combination (parallel and serial arrangements) of aerodynamic and sedimentary resistances within the layers and between adjacent layers, and resistances against impaction on the plant surfaces.

The forest parameterization within the model is set through the sizes and structures of the vegetation surfaces in each layer. The vertical structure of projected LAI and projected SAI are displayed in Fig. 1. The total LAI is 5.3, and the total projected SAI is 6.44. The total surface area per ground area is $17.2 \text{ m}^2 \text{ m}^{-2}$. As no data were available about the frequency distribution of twigs of different sizes, the original distribution of the spruce forest after Pahl (1996) was used. The meteorological driver of the model consists of the wind speed as measured directly above the canopy (21 m a.g.l.), the LWC of the cloud, and the fog droplet size distribution. Whenever directly measured data about the LWC and the drop size spectrum are not available, the data were estimated from the measured visibility as indicator for the density of the fog, as described in Section 3.1.

2.3. Direct flux measurement

We apply the eddy covariance concept to derive estimates of the turbulent fog water exchange above the top of a forest canopy. The direct measurement of vertical exchange fluxes of fog water, using micrometeorological techniques (including eddy covariance) from a single experimental tower, is feasible only within the limits set by the validity of assumptions concerning the flow field and energy fluxes at and above the canopy top. The mass balance for LWC is

$$\begin{aligned} \frac{\delta \overline{\text{LWC}}}{\delta t} = & - \sum_{j=1}^3 \overline{u_j} \cdot \frac{\delta \overline{\text{LWC}}}{\delta x_j} - \sum_{j=1}^3 \frac{\delta \overline{u_j \text{LWC}'}}{\delta x_j} \\ & + \frac{\delta v_s \cdot \overline{\text{LWC}}}{\delta x_3} + \overline{S_{\text{LWC}}}, \end{aligned} \quad (2)$$

where u_j is the wind component of the j th axis x_j of the Cartesian coordinate system, v_s is the deposition velocity, and S_{LWC} is the source and sink term for LWC. The first term on the right-hand side is the advection term. The effects of advection on eddy covariance estimates of surface exchange are only beginning to be understood

(Aubinet et al., 2003; Feigenwinter et al., 2004). Although advection is usually attributed to terrain inhomogeneity, in the case of fog water and sloping terrain, it can exist even for a perfectly homogeneous surface because of the relationship between altitude and phase change (see discussion of the last term in Eq. (2) below). Another potential source of error is entrainment (Businger, 1986), particularly at the edges and close to the tops and bottoms of clouds within the mountain ranges. However, for our study, no data from other sites upwind or downwind are available. Horizontal advective processes have to be neglected, so that our study is a purely one-dimensional approach to fog water exchange. This is in conceptual agreement to the Lovett model, which is one-dimensional as well. However, the error potential introduced with this assumption may have to be considered during interpretation of our results. For the vertical component x_3 , the average of the wind component u_3 , which will be called \bar{w} hereafter, is zero within the experimental frame. Data subsets with too large values (positive or negative) of \bar{w} were excluded from further processing through the routine quality assurance procedure (Foken and Wichura, 1996).

The second term on the right-hand side of Eq. (2) is the turbulent flux. The horizontal terms of the horizontal flux are neglected with the same arguments given for the advective terms, with the additional justification through the estimate that the turbulent contribution is even much smaller than the advective one.

The third term is the sedimentation (or gravitational settling) of fog droplets. This process must not be neglected when estimating the vertical fluxes of fog water and will be detailed below.

The fourth term on the right-hand side of Eq. (2) describes sources and sinks of fog water. The primary difficulty is that LWC and droplets are not conserved atmospheric scalars. It has been recognized that, when dealing with an atmospheric constituent that can change via chemical reactions (e.g., Lenschow, 1982; Kramm et al., 1995) one must account for atmospheric processes that can modify the flux between the surface and the point of measurement. This is true for thermodynamic transformations like phase changes. For example in conditions when solar radiation penetrates the cloud and heats the surface, diabatic heating of the surface and near-surface air may lead to evaporation of fog droplets. Therefore, evaporation can occur simultaneously with deposition (Unsworth, 1984). Vertical flux divergences of LWC have been observed at our site (Burkard et al., 2002), and evaporation and condensation of fog droplets are prime candidates to have caused these effects. For the present study, the condensational or evaporative sink is neglected. This is, again, in conceptual agreement with the Lovett model, where this process is not implemented. However, caution must be applied during data analysis and interpretation.

Now we introduce F_{tot} as the total exchange flux of fog water at the canopy top. With the simplifying assumptions, this flux is one-dimensional (vertical). After integration of Eq. (2) over the height of the measurement over the displacement height, F_{tot} is the sum of the turbulent exchange flux of fog water, $F_{\text{t,fog}}$ and the sedimentational flux, $F_{\text{s,fog}}$.

$$F_{\text{tot}} = F_{\text{t,fog}} + F_{\text{s,fog}}, \quad (3)$$

with $F_{\text{t,fog}}$ being the covariance of the vertical wind component w and LWC

$$F_{\text{t,fog}} = \overline{w' \cdot \text{LWC}'}, \quad (4)$$

where w' is the deviation from the mean of the vertical wind component w , and LWC' the deviation from the mean of the LWC, and the overbar indicates the arithmetic mean over the integration period (30 min). Eq. (4) is the eddy covariance expression for LWC.

The turbulent deposition of fog water was directly measured with the eddy covariance technique. The setup and data processing routines are described in Burkard et al. (2002) and Wrzesinsky (2004) and are only briefly outlined here. Similar setups have been applied by Kowalski et al. (1997) and Beswick et al. (1991). In our application, wind and droplet size distributions were measured with a Young 81000 ultrasonic anemometer and a fast droplet spectrometer FM-100 (Droplet Measurement Technologies, Inc.), which is a further development of the Forward Scattering Spectrometer Probe (FSSP, e.g. Brenguier et al., 1998). The data collection rate f was 8.6 Hz in the year 2000 and 12.5 Hz in 2001 and 2002, respectively. Droplet size distributions were measured in $i = 40$ size channels for diameters up to 50 μm . In principle, Eq. (2) or, in the simplified form, Eqs. (3) and (4) have to be applied for each size class channel and each time period separately and be added up to compute the total flux. Potential migration of individual droplets between size channels due to evaporation or condensation would have to be treated with the last term in Eq. (2), which however has been omitted here for simplicity. In our operational routine, the total LWC was computed from the droplet size spectrum, and the turbulent deposition flux $F_{\text{t,fog}}$ was computed for 30-min intervals by directly applying Eq. (4) for each time step.

The sedimentation, i.e. gravitational fluxes $F_{\text{s,fog}}$, could not be directly measured and were thus calculated from Stokes' law. In this case, a calculation for each of the 40 size channels had to be realized because the sedimentation velocity varies largely with droplet size:

$$F_{\text{s,fog}} = \sum_i v_{\text{s},i} \cdot \text{LWC}_i, \quad (5)$$

where $v_{\text{s},i}$ is the sedimentation velocity and LWC_i the liquid water content of the i th size channel of the measured droplet size distribution, respectively.

The sedimentation velocities are calculated as

$$v_{\text{s},i} = \frac{g \cdot D_i^2 \cdot (\rho_w - \rho_a)}{18 \cdot \eta_a}, \quad (6)$$

with g being the gravitational acceleration, D_i the mean droplet diameter of the i th size class, ρ_w and ρ_a the densities of liquid water and air, respectively, and η_a the viscosity of air. The total deposition flux of fog, F_{tot} , was computed as the sum of $F_{\text{t,fog}}$ and $F_{\text{s,fog}}$ (Eq. (3)). The turbulent flux $F_{\text{t,fog}}$ is considerably larger than the sedimentary flux $F_{\text{s,fog}}$ (see Section 3.5).

2.4. Experimental periods

At the research site "Waldstein", the chemistry and physics of fog had been measured since the summer of 1997 (Wrzesinsky and Klemm, 2000). Fog exchange studies were established later. The eddy covariance method was operated for two extended time periods from 18 September 2000 through 05 December 2000, and from 17 April 2001 through 18 March 2002, respectively. For these times, inter-comparisons between the deposition model and the direct exchange measurements are possible. Data for the model operation (i.e. wind speed at 21 m a.g.l. and visibility) are available for longer periods. We use the data set from January 1998 through August 2002 to present model results in Section 3.7.

3. Results and discussion

Before presenting comparisons between measured turbulent exchange and modelled fog deposition in Sections 3.5 and 3.7, we analyze the parameters that drive the model and estimate the uncertainties involved in measurement and model approaches.

3.1. Liquid water content and droplet size distribution

Depending on the availability of measured data, the model may be operated in three various modes: (1) With measured data of the DSD, the model can be directly driven. (2) If data of the LWC are available, the DSD can be parameterized from these data. (3) If only VIS data are available, LWC must be estimated plus the DSD has to be parameterized from LWC. For the times of deposition measurements at our site, LWC and DSD are available and option (1) can be applied. We did not use this option, but utilized the measured DSD and resulting LWC to derive parameterizations of DSD from LWC data (option (2), for details see below).

For the operation of the model for times when only VIS data are available, and for a more general evaluation of the model performance, option (3) has

been applied. For the parameterization of LWC (in g m^{-3}) from measured VIS (in m) data, Pahl (1996) used a potential equation of the form

$$\text{LWC} = a \times \left(\frac{\text{VIS}}{\text{m}}\right)^{-b}, \tag{7}$$

with $a = 38.91 \text{ g m}^{-3}$ and $b = 1.15$ (non-dimensional). For our site, we found that the parameters $a = 171.4 \text{ g m}^{-3}$ and $b = 1.45$ yield better results, but the differences for these two parameter sets were of minor importance. As visibilities below $\text{VIS} = 100 \text{ m}$ rarely occurred, a separate parameterization for these conditions was not needed. Fig. 2 shows that there is a large scatter between LWC and VIS. In particular for visibilities below $\text{VIS} = 200 \text{ m}$, the LWC for a given VIS may vary by a factor of up to 5.

For the modelling of the DSD from LWC data, Lovett (1984) used a unimodal function after Best

(1951). Pahl (1996) used a trimodal function after Deirmendjian (1969) because it yielded a better approximation to her data from the German mountain range. We found for our data set, that the addition of two log-normal distributions yielded the best approximation to our data:

$$\text{LWC}(r) = a \times \exp\left(-\frac{(\log_{10}(D/2 \mu\text{m}) - b)^2}{c^2}\right) + d \times \exp\left(-\frac{(\log_{10}(D/2 \mu\text{m}) - e)^2}{f^2}\right). \tag{8}$$

This was the best way to represent both the maximum of the frequency distribution between 7 and $10 \mu\text{m}$ diameter, and the relatively high importance of droplets with diameters larger than $D = 10 \mu\text{m}$. The parameterization of the size distribution was performed for eight LWC classes. The classes and the computed constants are shown in Table 1. Fig. 3 shows the data for the third LWC class ($0.2 \text{ g m}^{-3} < \text{LWC} < 0.3 \text{ g m}^{-3}$), and the three parameterizations as discussed above. It becomes evident that the sum of two log-normal distributions yields the best fit to the original data set. However, it also becomes evident that the scatter of the frequency distribution is large, so that the approximation of the droplet size distribution of an individual event may be poor even with this approximation.

3.2. Wind speed profile

One key driver of the model is the horizontal wind speed at the canopy top. The model reacts virtually linearly to changes of the wind speed: A doubling of the wind speed almost doubles the modelled deposition flux. This high sensitivity is due to the high relative importance of turbulent deposition, as compared to sedimentary flux at our mountainous site. It is therefore of crucial importance to use high-quality wind speed data to drive the model.

The model creates its own wind speed profile within the forest stand by using the SAI distribution (c.f. Fig. 1).

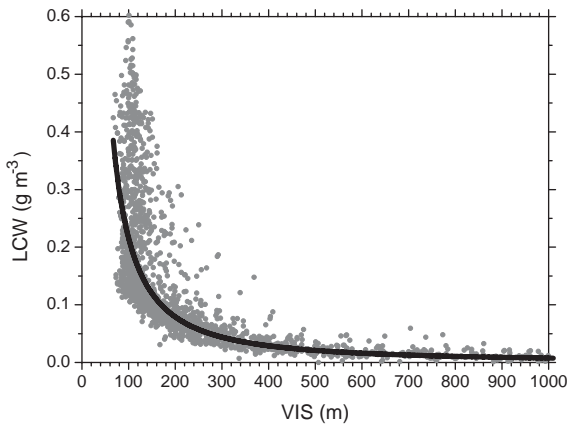


Fig. 2. Fog liquid water content (LWC) versus visibility (VIS) during the period 03 November 2000 through 05 December 2000 at the Waldstein research site. Dots represent 30 min averages. The full line represents the parameterization after Eq. (7).

Table 1
Parameters for the approximation of the double log-normal equation (Eq. (8)) for eight LWC classes at the Waldstein site

LWC class (g m^{-3})	a (g m^{-3})	b	c	d (g m^{-3})	e	f
0.025–0.1	0.008	0.722	0.167	0.001	0.798	0.415
0.1–0.2	0.021	0.769	0.176	0.006	0.809	0.304
0.2–0.3	0.039	0.823	0.186	0.003	0.837	0.514
0.3–0.4	0.050	0.857	0.186	0.003	0.889	0.529
0.4–0.5	0.044	0.893	0.167	0.018	0.917	0.312
0.5–0.6	0.064	0.926	0.201	0.006	2.911	2.122
0.6–0.7	0.064	0.951	0.183	0.010	1.079	0.521
0.7–0.8	0.039	0.996	0.339	0.027	1.013	0.154

The parameters b , c , e , and f , are dimensionless.

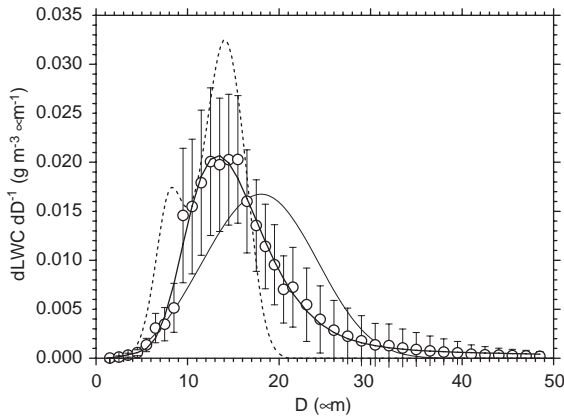


Fig. 3. Fog droplet size distribution for the time period April 2001 through March 2002 for the LWC class $0.2 \text{ g m}^{-3} < \text{LWC} < 0.3 \text{ g m}^{-3}$. Open bullets represent the measured means with standard deviation indicated. The thin full line is the approximation after Best (1951), the dotted line is the approximation after Deirmendjian (1969), and the bold full line is the sum of two log-normal distributions (Eq. (8)).

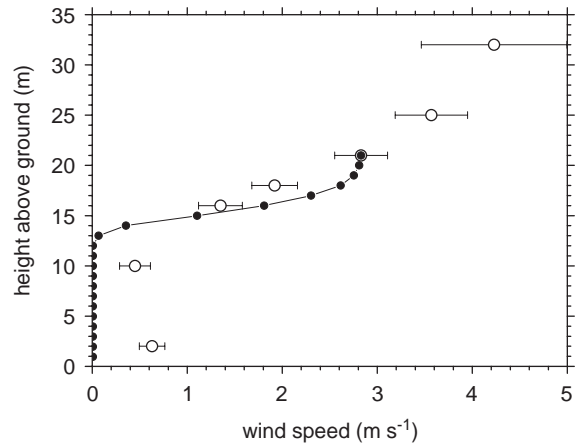


Fig. 4. Average measured and modelled wind speed profile in the Norway spruce forest. Full symbols represent the profile as computed with the fog deposition model. Open symbols are averages of all measurements during a 13-day period in summer 2001 with wind speed between 2.5 and 3.5 m s^{-1} at the 21 m level ($n = 76$, bars indicate single standard deviations). The wind speed of the model at 21 m above ground is set to 2.83 m s^{-1} to match the measured average.

Fig. 4 shows the modelled wind speed profile within our spruce forest in comparison to the measured one with identical wind speed at 21 m a.g.l. The model predicts a strong decrease of the wind speed between 19 and 14 m a.g.l. , with zero wind speed at altitudes below 12 m a.g.l. The measured profile is logarithmic above the canopy (between 21 and 32 m), exhibits a minimum at the range where the model drops to zero, but the wind speed increases at heights closer to the ground. This is an indication of lateral advection of air into the trunk space. If this air carries significant LWC, it might contribute to the deposition of fog within the trunk space. This potential error would neither be detected by the measurements nor by the model, and would therefore not affect the comparability of these approaches. In addition the actual experience and observations during frequent visits at the field site do not support the hypothesis that high LWC is present in the trunk space.

3.3. Uncertainty analysis

Both measurements and models are associated with uncertainties from various sources. In each approach (measurement and model), the vertical transport of liquid water is quantified at one point in space, and the results are extrapolated and interpreted as area-averaged exchange fluxes of fog water between the vegetation and the adjacent atmosphere (always deposition for the model). To the degree that these fluxes vary with space, the extrapolation is invalid. Extensive analyses of the turbulence structure during deposition measurements of

ozone (Klemm and Mangold, 2001) and within the fog deposition measurements (Wrzesinsky, 2004) showed that mechanical disturbances from in-homogeneities of the terrain or the vegetation do not occur for most of the time. Times when disturbances were detected (for example during wind directions from the tower to the experimental set up) were excluded from further data analysis. Due to the high quality of experimental data we assume that the one-dimensional model is applicable to the forest as well.

Burkard et al. (2002) detected a vertical divergence of the turbulent fog water flux at this site between the levels of 32 and 22 m above ground, respectively. The turbulent deposition fluxes at 22 m were, on average, by 45% smaller than those at 31.5 m . Similar results were reported by Kowalski and Vong (1999) for a different site. The most likely explanation for this observed phenomenon at our site is evaporation of droplets during the deposition process (Burkard et al., 2002). Evaporation of droplets is identified by the last term on the right-hand side of Eq. (2). However, this term is neglected in our computation of fluxes from eddy covariance data (Eqs. (3) and (4)). In the model, the process of evaporation as possible source of flux divergence is not included either. The eddy covariance measurements rely on data that were collected at 32 m above ground, the model data mostly refer to the height of 21 m . Therefore, an overestimate of measured over modelled deposition fluxes may partly be due to flux divergences.

In Section 3.6, we compare measured and modelled results on a monthly basis. Uncertainty in these results, resulting from counting statistics of the FM 100 and from uncertainty in the vertical wind measurements, are determined following suggestions given by Buzorius et al. (2003). For each 30-min interval, the statistical uncertainty from droplet counting, $dF_{\text{count},i}$ is determined for each droplet size class as

$$dF_{\text{count},i} = \frac{\sigma_w \cdot \text{LWC}_i}{\sqrt{N}}, \quad (9)$$

with σ_w being the standard deviation of the measured vertical wind speed w , and N the number of droplets per size class i . The uncertainty from the vertical wind measurement dF_w is calculated as

$$dF_w = \sqrt{\frac{\text{LWC}^2 \cdot (dw)^2}{f \cdot T}}, \quad (10)$$

with dw being the uncertainty of the vertical wind speed measurement ($dw = 0.05 \text{ m s}^{-1}$), f the data collection rate (8.6 or 12.5 Hz), and T the duration of the collection interval (1800 s). The uncertainties for each collection interval and for the monthly depositions are computed from the respective $dF_{\text{count},i}$ and dF_w values, following the rules of error propagation in addition routines.

For the model, the uncertainty analysis follows the concept of the basic model equation (Eq. (1)) in the modified form

$$F_{\text{tot}} = \text{LWC} \times v_d, \quad (11)$$

with v_d being the deposition velocity ($v_d = 1/R_{\text{tot}}$), assuming that the uncertainties for the LWC estimate and for the deposition velocity are combined through the multiplication. A major driver for the deposition velocity is the horizontal wind speed. The modelled deposition velocity responds directly and linearly to the wind speed (see also Section 3.2). Therefore, we use the uncertainty of the horizontal wind speed measurement as a proxy of the uncertainty of the deposition velocity.

For the estimate of the uncertainty of LWC, two independent approaches were used for the VIS version and for the DSD version of the model, respectively. For the VIS version, the measured visibilities were classified into 24 classes. Fifty-meter steps were used for $50 \text{ m} < \text{VIS} < 500 \text{ m}$, and 100-m-steps were used for $500 \text{ m} < \text{VIS} < 2000 \text{ m}$, respectively ($\text{VIS} < 50 \text{ m}$ did not occur, $\text{VIS} > 2000 \text{ m}$ did not contribute to liquid water deposition). For each visibility class, the confidence interval of all measured LWC values (c.f., Fig. 2) was computed and used as estimator for all individual VIS values within the class. For the DSD version, we utilized the regression of 1516 pairs of LWC measurements (30-min averages) using a FM100 spectrometer and a PVM monitor (Gerber et al., 1999) that were collected on a

mountain site in Switzerland (Burkard, pers. commun., 2002). The squared regression coefficient was $r^2 = 0.8874$, with a standard error of the slope of 0.00755 and a standard error of intercept of 0.7471 mg m^{-3} LWC. From these data, the 95% confidence interval of the LWC measurement of our FM100 was computed.

3.4. Modelled versus measured turbulent exchange deposition—single day and event analysis

The comparison of turbulent fog water fluxes $F_{\text{t,fog}}$ as quantified with the Lovett model and with the eddy covariance measurements exhibits varying results from event to event. Examples of two different experimental days are displayed in Fig. 5. For the Lovett model, the version using parameterized DSD, with the sum of two log-normal distributions (Eq. (8)), is used for this comparison. On 28 October 2001 (left panels in Fig. 5), dense fog was present before about 04 h and after 22 h. During these periods, deposition of fog occurred in the model and in the measurements. The model deposition was larger by about 0.13 mm or 18% than the measured deposition. For the time between 04 and 11 h, positive and negative fluxes occurred in the measurements, the latter indicating a measured upward fog water flux. For this time period, the net flux as measured was about zero. At the same time, the model yielded a deposition flux of 0.1 mm. For the entire day, the cumulative deposition flux was 0.94 mm and thus by 0.22 mm or 31% larger than the measured one. The scatter plot between these two data sets shows a significant regression ($r^2 = 0.973$) with slope 0.86.

On 28 October 2001 (right hand panels in Fig. 5) the situation is very different. Dense fog ($\text{VIS} < 500 \text{ m}$; most of the time $\text{VIS} < 100 \text{ m}$) occurred throughout the day. Considerable deposition fluxes occurred in model and measurements. The measured deposition was by 0.13 mm or 16% larger than the modelled one. The lower right panel in Fig. 5 shows that some of the measured data points are zero. These data did not pass the quality assurance procedure (for stationarity and friction velocity restrictions) and therefore had to be set zero. The regression of the measured versus modelled fluxes (excluding the data points of measurement = 0) yields a regression with $r^2 = 0.89$ and slope 0.98.

The scatter between the modelled and measured fog water fluxes as analyzed on single event basis is large. Ensemble analysis was performed for all events between April 2001 and March 2002. For 15 out of 260 events, the measured fluxes were upward. Most of these upward fluxes were below 0.01 mm. Further comparisons were performed for those events when both the measured and the modelled deposition fluxes were larger than 0.01 mm. For 60% of these 197 events, the measured flux was smaller than the modelled one. The median of the ratio

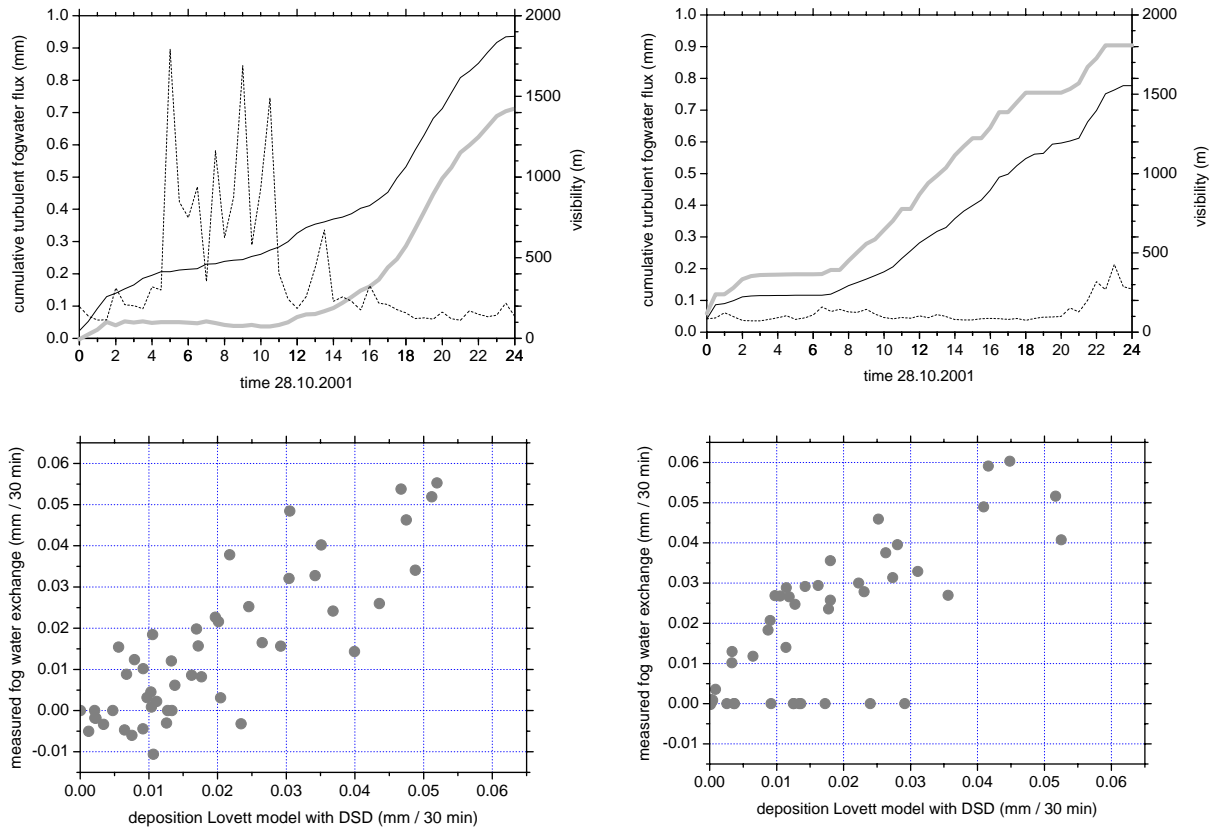


Fig. 5. Turbulent fog water fluxes as compared between the Lovett model (with DSD) and the eddy covariance measurements. 30-minute averages are shown. Top panels: Cumulative fluxes for 28 October 2001 (left panel) and 20 February 2002 (right panel). The black lines show the Lovett model results, the bold grey lines the eddy covariance measurements. The broken lines indicate the visibility. Bottom panels: Scatter plots of measured (eddy covariance) versus modelled (Lovett model with DSD) turbulent fluxes for 28 October 2001 (left) and 20 February 2002 (right).

measured/modelled deposition flux was 0.76, 50% of the ratios were between 0.31 and 1.59, 90% of the ratios were between 0.08 and 4.6. Data filtering into LWC classes, friction velocity classes, or along other parameters, did not change the picture significantly (results not shown). These results show that the scatter between modelled and measured turbulent exchange of fog water is large on single event basis. As we are interested in the quantification of fog water deposition over longer time periods, we merged the data into monthly ensembles and continued the comparison of model with measurements on the basis of these data (Section 3.6).

3.5. Sedimentation fluxes

The sedimentation (gravitational settling) of fog droplet is quantified in both the one-dimensional model and the “direct measurement” through computation following Stokes’ law. The model computed the settling

to any surface in each of the layers within the forest, whereas the “measurement” computes simply the gravitational flux through the balance layer above the tree top. Overall, the model yields sedimentary fluxes that are approximately 50% higher than those of the “measurement”. The contribution of sedimentary fluxes to total fog fluxes is up to 20% in the model. These differences of sedimentation fluxes between model and measurement are small in comparison to those of the turbulent fluxes. Therefore, the comparisons as discussed below mainly refer to the turbulent fluxes of fog droplets.

3.6. Modelled versus measured deposition—monthly analyses

For the reasons outlined in Section 3.4 we compare the modelled with measured depositions on a monthly basis. For this comparison, two model versions are used:

One employs the parameterized DSD (see Section 3.4 and Fig. 2). For further applications of the model also for conditions when no DSD data are available, the model version employing the measured VIS data (Eq. (7)) as input are also compared.

The 95% confidence intervals were calculated as described in Section 3.3. The results are presented in Fig. 6. The measured fog water flux is in all cases a deposition flux. It becomes evident that for the period from September through December 2000, the modelled depositions are significantly larger than the measured ones. The monthly surplus of the modelled over the measured deposition is between 90% and 200% for the model with use of the measured DSD, and between 50% and 310% for the model with use of measured VIS data. The 95% confidence intervals of the measurement on the one hand and the model on the other hand do not overlap. In total of this first experimental phase, the model significantly yields higher deposition estimates, by a factor of 2.0 (with DSD) or 2.3 (with VIS), respectively.

For the second, longer experimental period from April 2001 through March 2002, the picture is less clear. For the time period between May 2001 and March 2002, the deposition as modelled with DSD is between -30% and $+126\%$, as compared to the measurement. A

negative deviation occurred only during one month (January 2002), the average deviation is $+40\%$. It is quite striking that the 95% confidence intervals between the measurement and the model with DSD overlap each other only for 2 months (August 2001 and February 2002). This shows that the deviations between these numbers are statistically highly significant for most of the time.

For the model with VIS, most deviations with the measurements (9 out of 11 monthly means between May 2001 and March 2002) are negative, with the average over this time period being -26% . The 95% confidence intervals of the model with VIS are generally much larger than those of the model with DSD. This results from the high uncertainty of LWC estimate from visibility data. As a consequence, the intervals of the model with VIS on the one hand and measurement on the other hand overlap for three months (August 2001, December 2001, February 2002).

Combining the sums of deposition estimates of both experimental periods, the measured deposition is 139 mm. In comparison, the deposition modelled with DSD was 190 mm or 37% higher than the measured deposition. The modelled deposition with VIS was 106 mm or 24% less than the measurement. For neither of the models, the 95% confidence interval overlaps with the respective interval of the measurement, indicating statistical confidence in the conclusion that models and measurements do not agree.

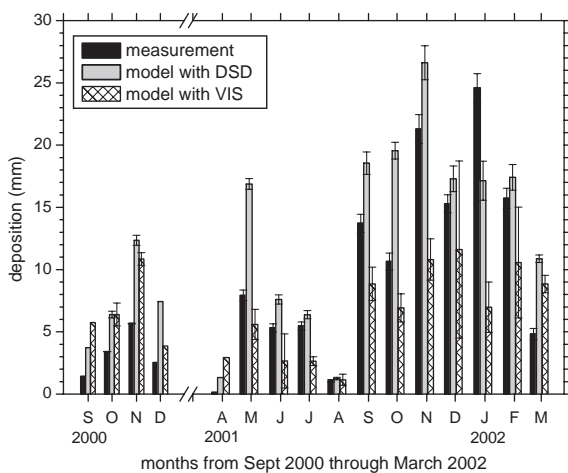


Fig. 6. Monthly deposition of fog water for the experimental periods in 2000 and 2001/2002, given in units mm, which is equivalent to liters per square meters ($l m^{-2}$) ground area. Note that the months at the beginnings and ends of experimental periods are not complete. However, the integration times for model and measurements are synchronous. The sums for the two experimental periods are given in Table 2. Error bars represent 95% confidence intervals based on the analyses described in Section 3.3. For September 2000, December 2000, and April 2001, no confidence intervals were computed because less than 15 days of these months were covered by the measurements, respectively.

3.7. Long term model application

Fig. 7 shows the fog deposition on a monthly basis, as modelled by using the VIS data, from January 1998 through August 2002. It becomes evident from these

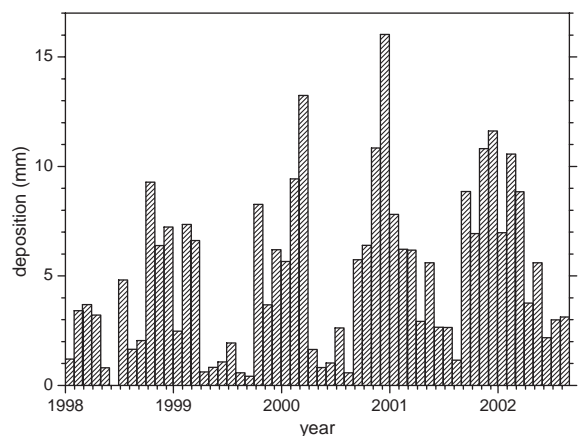


Fig. 7. Monthly deposition of fog water as modelled for the period from January 1998 through August 2002, using the VIS data. For June 1998, no VIS data are available.

Table 2
Measured and modelled total fog deposition (mm or lm^{-2}) during the two field periods

Period	Measured	Modelled with DSD	Modelled with VIS
09/2000–12/2000	13.0	29.9	26.8
04/2001–03/2002	126	161	79.6

Data are sums of the respective data subsets in Fig. 5.

results that the fog deposition is much higher in winter as compared to the summer periods, typically the period from April through August, respectively. However, the results in Fig. 7 must be interpreted with care. Deviations for single months have been shown to be between -18 and $+5$ mm. For longer integration periods of several months (see Table 2), the deviations may be almost as large as -40% or $+100\%$.

4. Conclusions

We studied fog water fluxes at a canopy top in a mountainous region of Central Europe. The scope of this study was to compare a well-established one-dimensional model with direct measurements of turbulent fluxes with the eddy covariance technique. The overall goal is the quantification of fog deposition on larger time scales in order to further evaluate the role of fog in the hydrological and biogeochemical cycles of the ecosystem.

A major point of concern lies in the one-dimensionality of both the model and the experimental approach. Advective fluxes above the canopy may influence the mass balance in the atmospheric layer between the canopy top and the height of measurement. These effects were excluded from our analysis. Potential impact on the results would affect both the model and the measurements and probably have a minor effect on the comparison between the two.

A second issue is the potential non-closure of the mass balance for LWC in cases when evaporation or condensation occurs. Vertical flux divergences of LWC have been observed at our site (Burkard et al., 2002) for measurement heights of 32 and 22 m above ground, respectively. These effects are important to consider when the input of LWC to the ecosystem through fog deposition is evaluated from a hydrological point of view. In the present comparison, eddy covariance fluxes were quantified at 32 m above ground, while important input parameters for the Lovett model were measured at 21 m (wind) and 25 m (visibility) above ground (not

LWC for parameterization of the DSD, these data refer to 32 m). Any systematic underestimation of modelled deposition flux (in particular those using VIS data) with respect to measured depositions in the order of tens of percent may be partly due to the flux divergence.

Eddy covariance measurements of turbulent fluxes of fog droplets are anything but routine. The fog droplet monitor FM100, which is capable of measuring size spectra of fog droplets with diameters between 2 and $50 \mu\text{m}$ (40 size classes) with about 10 Hz temporal resolutions, operated well throughout the experimental phases (summer and winter). However, restrictions to the applicability of the eddy covariance assumptions (stationarity of the flow field, establishment of highly turbulent conditions) occurred. This led to rejection of flux data through the quality assurance routine. As the rejected data points were set to zero (and no gap-filling routine was applied), this leads to a potential underestimation of the deposition flux of LWC to the ecosystem.

The Lovett model (Lovett, 1984; Pahl, 1996) was operated in two different modes: First, by use of the DSD as parameterized from measurements, and secondly by use of the measured VIS as indicator for the density of fog. The drawback of the latter method is the fact that the LWC and DSD of the fog have to be parameterized, the advantage is that it requires less sophisticated input data and is therefore better suited for long term operation. The use of the DSD in the model should yield better quality results than the use of VIS data, because the model requires less parameterization in that case.

In the direct comparison of the turbulent flux from the model with that from the eddy covariance measurements on a daily or event basis, the agreement is within about $\pm 60\%$ for half of the events. Larger relative disagreements occur when the absolute fluxes are low, or when the database for the eddy covariance measurements is reduced by the quality assurance routine. In our view, the highest value of our comparison lies in the analysis of long term data set, aiming at answering the questions: How large is the deposition of fog water to the ecosystem? How large is the deposition of solutes (such as pollutants or nutrients)? Which are appropriate tools to quantify these deposition fluxes?

For the quantification of long-term (deposition) fluxes, both in the model and in the “measurement”, the sedimentation flux (Section 3.5) has to be included.

In comparison with the measured deposition, the predicted fog deposition using DSD is higher. This holds for the entire data set (deviation $+37\%$) and for most single months (with exemption of January 2002). The 95% confidence intervals, which quantify uncertainties that originate from variations of the measured input parameters, do not overlap for most months. This shows that the deviations between the measured and modelled (with DSD) fog water deposition differ significantly.

The agreement between model and measurement appears to be better if VIS data are used as model input to parameterize LWC. In this case, the model estimates lower deposition than the measurement (–23% for the entire data set). These deviations may originate from flux divergences within the 10 m atmospheric layer above the canopy top. On the other hand, the uncertainties of the model using VIS are larger than for those using the DSD data. This originates in the large scatter of the correlation between LWC and VIS (Fig. 2).

In conclusion we found that the agreement between model and measurement is generally poor. However, the model is able to predict the order of magnitude of the fog deposition. Depending on the question to be studied, the model may be of use. Within these limits, the use of VIS as model input parameter seems appropriate.

The importance of fog deposition lies mainly in the input of nutrients and pollutants through fog deposition, because the solute concentrations in fog are much higher than those in rain. For some ions, the enrichment in fog water over-compensates the small contribution in the water balance, meaning that more deposition takes place through fog than through rain and snow. Therefore, fog deposition plays a very important role in the biogeochemical cycles of nutrients and forest fertilization through atmospheric deposition, in particular for nitrogen containing compounds. The LWC flux divergence that was observed at our site does not affect the interpretation of fluxes of ions or other compounds of fog water, because evaporation and condensation does not influence the total amount of these fog water compounds per air volume (Burkard et al., 2002).

In our opinion, the deposition of pollutants and nutrients through fog to various ecosystems deserves further studies. In particular for mountain ecosystems, far too little is known about the magnitude, temporal and spatial variability of fog deposition and its driving forces. Given the uncertainties in the widely used one-dimensional model, we suggest that more direct measurements of fog deposition should be undertaken in mountainous ecosystems of the world.

Acknowledgments

These studies were supported by the German Science Foundation (DFG) through Grants KL 623/4 and by the German Federal Research Ministry (BMBF) through Grant PT-BEO 51–0339476D. We thank J. Gerchau for help during the field campaigns. The cooperation of P. Winkler (Deutscher Wetterdienst, Hohenpeißenberg) by sharing an operational version of the fog deposition model with us is gratefully acknowledged. The manuscript also gained largely from helpful comments by three anonymous reviewers.

References

- Alsheimer, M., 1996. Xylemflußmessungen zur Charakterisierung raumzeitlicher Heterogenitäten in der Transpiration montaner Fichtenbestände (*Picea abies* (L.) KARST.). Bayreuther Forum Ökologie 46, 1–143.
- Aubinet, M., Heinesch, B., Yernaux, M., 2003. Horizontal and vertical CO₂ advection in a sloping forest. *Boundary-Layer Meteorology* 108, 397–417.
- Baumgardner, R.E., Isil, S.S., Lavery, T.F., Rogers, C.M., Mohnen, V.M., 2003. Estimates of Cloud Water Deposition at Mountain Acid Deposition Program sites in the Appalachian Mountains. *Journal of Air and Waste Management Association* 53, 291–308.
- Baumgartner, A., 1958. Nebel und Niederschlag als Standortfaktor am Großen Falkenstein (Bayrischer Wald) Forstwiss. *Centralblatt* 13, 257–272.
- Baumgartner, A., 1959. Das Wasserangebot aus Regen und Nebel sowie die Schneeverteilung in den Wäldern am Großen Falkenstein (Bayrischer Wald). *Wald und Wasser* 3, 45–54.
- Best, A.C., 1951. Drop-Size Distribution in Cloud and Fog. *Quarterly Journal of the Royal Meteorological Society* 77, 418–426.
- Beswick, K.M., Hargreaves, K., Gallagher, M.W., Choularton, T.W., Fowler, D., 1991. Size-resolved measurements of cloud droplet deposition velocity to a forest canopy using an eddy correlation technique. *Quarterly Journal of the Royal Meteorological Society* 117, 623–645.
- Brenguier, J.L., Bourriane, T., de Araujo Coelho, A., Isbert, J., Peytavi, R., Trevarin, D., Weschler, P., 1998. Improvements of droplet size distribution measurements with the fast-FSSP (Forward Scattering Spectrometer Probe). *Journal of Atmospheric and Oceanic Technology* 15, 1077–1090.
- Burkard, R., Eugster, W., Wrzesinsky, T., Klemm, O., 2002. Vertical divergences of fogwater fluxes above a spruce forest. *Atmospheric Research* 64, 133–145.
- Businger, J.A., 1986. Evaluation of the accuracy with which dry deposition can be measured with current micrometeorological techniques. *Journal of Climate and Applied Meteorology* 25, 1100–1124.
- Buzorius, G., Rannik, Ü., Nilsson, E.D., Vesala, T., Kulmala, M., 2003. Analysis of measurement techniques to determine dry deposition velocities of aerosol particles with diameters less than 100 nm. *Journal of Atmospheric Science* 34, 747–764.
- Deirmendjian, D., 1969. *Electromagnetic Scattering on Spherical Polydispersions*. New York, Elsevier.
- Feigenwinter, C., Bernhofer, C., Vogt, R., 2004. The influence of advection on the short-term CO₂-budget in and above a forest canopy. *Boundary-Layer Meteorology* 113, 201–224.
- Foken, T., Wichura, B., 1996. Tools for quality assessment of surface-based flux measurements. *Agricultural and Forest Meteorology* 78, 83–105.
- Fowler, D., Morse, A.P., Gallagher, M., Choularton, T., 1990. Measurements of cloud water deposition on vegetation using a lysimeter and a flux gradient technique. *Tellus* 30, 285–293.
- Gerber, H., Frick, G., Rodi, A.R., 1999. Ground-based FSSP and PVM measurements of liquid water content. *Journal of Atmospheric and Oceanic Technology* 16, 1143–1149.

- Grunow, J., 1955. Der Nebelniederschlag im Bergwald. *Forstwissenschaftliches Centralblatt* 74, 21–36.
- Joslin, J.D., Mueller, S.F., Wolfe, M.H., 1990. Tests of models of cloudwater deposition to forest canopies using artificial and living collectors. *Atmospheric Environment* 24A, 3007–3019.
- Klemm, O., Lange, H., 1999. Trends of air pollution in the Fichtelgebirge Mountains, Bavaria. *Environmental Science and Pollution Research* 6, 193–199.
- Klemm, O., Mangold, A., 2001. Deposition of ozone at a forest site in NE Bavaria. *Water, Air, and Soil Pollution: Focus* 1, 223–232.
- Kowalski, A.S., 1997. Occult cloudwater deposition to a forest in complex terrain: Measurement and interpretation. Ph.D. thesis, Oregon State University, 208pp.
- Kowalski, A.S., Vong, R.J., 1999. Near-surface fluxes of cloud water evolve vertically. *Quarterly Journal of the Royal Meteorological Society* 125, 2663–2684.
- Kowalski, A.S., Anthoni, P.M., Vong, R.J., Delany, A.C., Maclean, G.D., 1997. Development and evaluation of a system for ground-based measurement of cloud liquid water turbulent fluxes. *Journal of Atmospheric and Oceanic Technology* 14, 468–479.
- Kramm, G., Dlugi, R., Dollard, G.J., Foken, T., Mölders, N., Müller, H., Seiler, W., Sievering, H., 1995. On the dry deposition of ozone and reactive nitrogen species. *Atmospheric Environment* 29, 3209–3231.
- Lenschow, D.H., 1982. Reactive trace species in the boundary layer from a micrometeorological perspective. *Journal of the Meteorological Society of Japan* 60, 472–480.
- Linke, F., 1916. Niederschlagsmessungen unter Bäumen. *Meteorologische Zeitschrift* 33, 140–141.
- Lovett, G., 1984. Rates and mechanisms of cloud water deposition to a subalpine balsam fir forest. *Atmospheric Environment* 18, 361–371.
- Lovett, G., Reiners, W., 1986. Canopy structure and cloud water deposition in a subalpine coniferous forest. *Tellus* 38B, 319–327.
- Marloth, H., 1906. Über Wassermengen welche Sträucher und Bäume aus treibendem Nebel und Wolken auffangen. *Meteorologische Zeitschrift* 23, 547–553.
- Matzner, E. (Ed.), 2004. *Temperate Forest Ecosystem Functioning in a Changing Environment—Watershed Studies in Germany*. Ecological Studies, vol. 172. Springer, Berlin.
- Mueller, S., 1991. Estimating cloud water deposition to subalpine spruce-fir forests I. Modifications to an existing model. *Atmospheric Environment* 25A, 1093–1104.
- Mueller, S., Joslin, L., Wolfe, M., 1991. Estimating cloud water deposition to subalpine spruce-fir forests II. Model testing. *Atmospheric Environment* 25A, 1105–1122.
- Pahl, S., 1996. *Feuchte Deposition auf Nadelwälder in den Hochlagen der Mittelgebirge*. Berichte des Deutschen Wetterdienstes, Offenbach.
- Pahl, S., Winkler, P., 1995. *Höhenabhängigkeit der Spurenstoffdeposition durch Wolken auf Wälder*. Abschlussbericht, Deutscher Wetterdienst, Meteorologischen Observatorium Hohenpeißenberg.
- Schulze, E.-D., Lange, O.L., Oren, R. (Eds.), 1989. *Forest Decline and Air Pollution: A Study of Spruce (Picea abies) on Acid Soils*. Ecological Studies, vol. 77. Springer, Berlin, p. 475pp.
- Tenhunen, J.D., Matzner, E., Heindl, B., Chiba, Y., Manderscheid, B., 2001. Assessing environmental influences on ecological function of a spruce forest catchment in the Fichtelgebirge. In: Tenhunen, J.D., Lenz, R., Hantschel, R. (Eds.), *Ecosystem Approaches to Landscape Management in Central Europe*, Ecological Studies, vol. 147. Springer, Heidelberg, pp. 357–375.
- Thalmann, E., Burkard, R., Wrzesinsky, T., Eugster, W., Klemm, O., 2002. Ion fluxes from fog and rain to an agricultural and a forest ecosystem in Europe. *Atmospheric Research* 64, 147–158.
- Trautner, F., Eiden, R., 1988. A measuring device to quantify deposition of fog water and ionic input by fog on small spruce trees. *Trees* 2, 92–95.
- Unsworth, M.H., 1984. Evaporation from forests in cloud enhances the effects of acid deposition. *Nature* 312, 262–264.
- US Environmental Protection Agency (EPA) (Ed.), 2000. *Cloud deposition to the Appalachian mountains 1994–1999*.
- Wrzesinsky, T., 2004. *Direkte Messung und Bewertung des nebelgebundenen Eintrags von Wasser und Spurenstoffen in ein montanes Ökosystem*. Dissertation Thesis, University of Bayreuth, 109pp. urn:nbn:de:bvb:703-opus-784.
- Wrzesinsky, T., Klemm, O., 2000. Summertime fog chemistry at a mountainous site in central Europe. *Atmospheric Environment* 34, 1487–1496.
- Wrzesinsky, T., Scheer, C., Klemm, O., 2004. Fog Deposition and its Role in Biogeochemical Cycles of Nutrients and Pollutants. In: Matzner, E. (Ed.), *Temperate forest ecosystem functioning in a changing environment—watershed studies in Germany*. Ecological Studies, vol. 172. Springer, Berlin, pp. 191–202.